BOLETIN DE LA SOCIEDAD ESPAÑOLA DE
Cerámica y Vidrio
www.elsevier.es/bsecv

Coercivity and morphology in Fe/NiO films deposited on nanoporous Al_2O_3 membranes

Enrique Navarro[a], *Francisco Javier Palomares*[a], *María Alonso*[a], *Federico Cebollada*[b,*], *Guillermo Dominguez-Cañizares*[c], *Alejandro Gutierrez*[c], *Leonardo Soriano*[c], *Jesús María González*[a]

[a] *Instituto de Ciencia de Materiales de Madrid (ICMM-CSIC), Cantoblanco, Madrid, Spain*
[b] *POEMMA, Dpto. Electrónica Física, ETSIT, Universidad Politécnica de Madrid, Madrid, Spain*
[c] *Dpto. Física Aplicada, Universidad Autónoma de Madrid (UAM), Cantoblanco, Madrid, Spain*

ARTICLE INFO

Article history:
Received 27 August 2015
Accepted 3 November 2015
Available online 12 November 2015

Keywords:
Magnetic properties
Thin films
Interfaces

ABSTRACT

The occurrence of ferro-antiferromagnetic (F/AF) interfaces in Fe/NiO bilayers brings about the possibility of controlling the Fe layer hysteretic properties through the unidirectional anisotropy induced by the presence of unbalanced, antiferromagnetic phase moments at that interface. In this work, we report on the Fe thickness and temperature dependencies of the hysteretic parameters measured in Fe/NiO bilayers deposited on Al_2O_3 nanoporous membranes. The Fe/NiO bilayers grew in a six-fold columnar way around each one of the membrane nanopores. The in-plane hysteresis loops measured by field cooling the samples down to different temperatures below 300 K, evidenced the occurrence of coercive forces larger than that associated to the Fe anisotropy field and also of significant loop shifts, both of them clearly linked to the occurrence of exchange bias at the Fe/NiO interfaces. The magnetization reversal mechanism active in the Fe/NiO bilayers essentially differs from that responsible for the reversal occurring in continuous films incorporating lithographed antidots, due to the fact that in our samples it does not involve either domain wall propagation or pinning, and the reversal events are spatially restricted to the Fe-covered, hexagonally closely packed dot-like tops of the NiO columns.

Coercitividad y morfología en películas de Fe/NiO depositadas sobre membranas porosas de Al_2O_3

Palabras clave:
Propiedades magnéticas
Láminas delgadas
Interfaces

RESUMEN

La presencia de intercaras ferro-antiferromagnéticas (F/AF) en bicapas de Fe/NiO permite modificar significativamente las propiedades de histéresis de la película de Fe mediante la anisotropía unidireccional, debido a la presencia de momentos de la fase antiferromagnética descompensados en la intercara. En este trabajo estudiamos la influencia del espesor de Fe y de la temperatura sobre los parámetros de histéresis de bicapas de Fe/NiO

* *Corresponding author.*
E-mail address: fcebollada@etsit.upm.es (F. Cebollada).
http://dx.doi.org/10.1016/j.bsecv.2015.11.001

depositadas sobre membranas porosas de Al_2O_3. Dichas bicapas crecen con estructura columnar hexagonal en torno a los poros de las membranas. Los ciclos de histéresis, medidos tras enfriar con campo a varias temperaturas por debajo de 300 K, han mostrado campos coercitivos mayores que los esperables considerando el campo de anisotropía del Fe y la existencia de desplazamientos de los ciclos hacia campos negativos, efectos ligados a la existencia de «*exchange bias*» en las intercaras Fe/NiO. El mecanismo de conmutación activo en las bicapas difiere del que tiene lugar en películas continuas litografiadas con «*antidots*». Ello es debido a que en nuestras muestras no se producen propagación y enganches de paredes y, además, a que la inversión de la imanación está espacialmente localizada en las estructuras de Fe tipo «*dot*» que recubren las columnas de NiO.

Introduction

It is well known that it is possible to get significant hardening of ferromagnetic phases in thin film form through both nano-patterning suitable motifs and nano-scale phase coupling [1,2]. The effects on nano-patterning can be exemplified by the hindering of the propagation of domain walls resulting from strong magnetostatic pinning centres introduced by engraving nano-metric hole (antidot) arrays on the film [3,4]. The second approach includes the so-called exchange bias effect, which gives also rise to a loop shift (usually) in the negative field sense. This effect is due to the coupling of the ferromagnetic (F) phase to an antiferromagnetic (AF) one and, more precisely, to the presence of unbalanced moments at the F/AF interface created by some type of local symmetry breaking at the antiferromagnetic phase [5]. Many different actual origins of those unbalanced moments have been identified, ranging from broken magnetic bonds to the presence of AF domain walls, but, as a general feature, the magnetic properties associated to the unbalanced moments (i.e. their magnitude and the local anisotropy, order temperature and stiffness constant corresponding to their coupling with the F phase moments) are only known to be distributed. Thus, it is difficult to design a general, efficient way of optimizing the hardening effect and this can only be achieved in a phenomenological way.

In this work we study the temperature dependence of the hysteretic properties of Fe/NiO bilayers grown onto anodized alumina membranes. Our aim was to explore the combined effects of the interfacial F/AF coupling and of the membrane morphology, which could limit either the linear dimensions of the structures mediating the magnetization reversal or effectively pin possible propagating structures. Particularly, we have considered thicknesses of the Fe layer which are slightly lower, similar and larger than the Fe (single crystal) correlation length (l_{ex} = 12 nm) [6].

Samples and experimental

Our samples were grown on top of anodic alumina membranes characterized by a distribution of closely packed pores with a diameter of 35 nm and an inter-pore average distance of 100 nm, which renders a porosity of ca. 11% as geometrically estimated. The deposition was initiated by the NiO layer and it was followed by the growth of a Fe deposit on top. The deposition of the NiO layers was carried out by rf magnetron sputtering from a NiO target [7]. The substrate was placed at a distance of 8 cm from the target, on a rotating sample-holder to ensure homogeneity. The magnetron

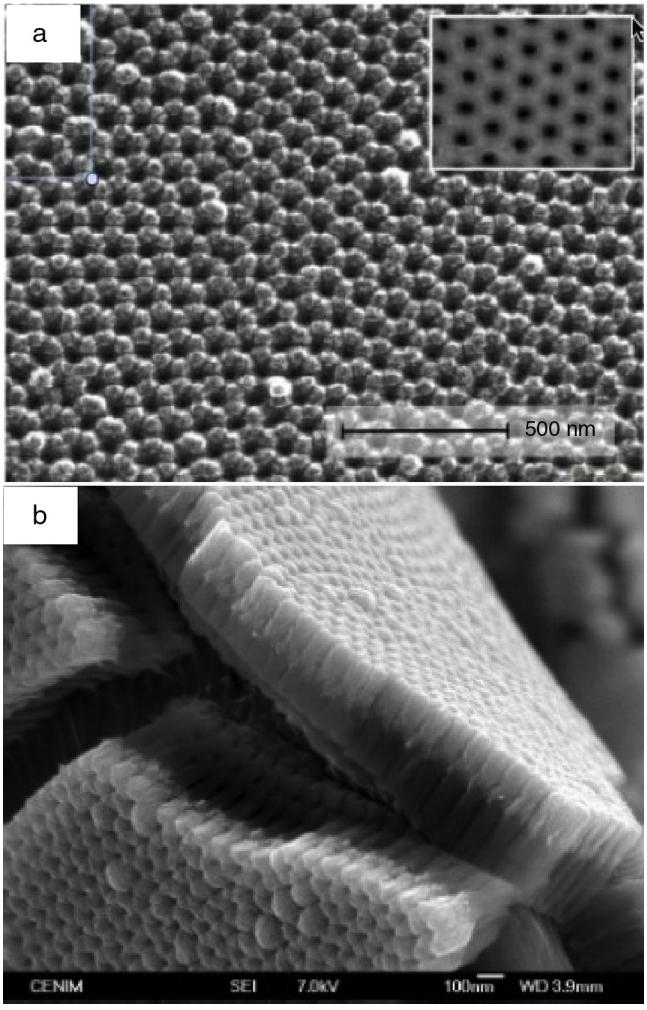

Fig. 1 – Top view of the NiO layer deposited on the alumina membrane (a) and fresh fracture image of the NiO/Al_2O_3 deposit (b); the upper, brighter region corresponds to the NiO layer.

power used was 100 W, and the pressure in the chamber was 2×10^{-2} mbar. The deposition time was 1 h in all cases. The NiO layers had an approximate thickness of 100 nm. The Fe layers were deposited using a pulsed laser deposition (PLD) device, with a base pressure of 10^{-10} mbar, working at 532 nm, 4 ns, 25 mJ pulses and 10 Hz pulse repetition frequency. The thicknesses of the Fe layers were 5 nm, 10 nm and 20 nm, respectively, and they were capped with a 10 nm thick Au layer.

The thickness of the NiO films was determined by a stylus profilometer (VeecoDektak 150). The morphology of the deposits (both NiO and the NiO/Fe bilayers) was examined by field emission scanning electron microscopy (FE-SEM) at 20 kV (Philips XL30 S-FEG with emission cathode) and Atomic Force Microscopy (AFM). The temperature dependence of the hysteretic properties was measured in the range from 300 K down to 50 K by means of a vibrating sample magnetometer and under fields of up to 4 T.

Results and discussion

Fig. 1(a) and (b) shows high-resolution SEM images of the NiO layer. As it can be seen in the top view of Fig. 1(a) the NiO growth preserves the hexagonal morphology of the alumina membranes. It also suggests the occurrence of polycrystalline nano-grains with contrasted crystallites, growing independently of one another. The cross section of the films, shown in Fig. 1(b), confirms that the six-fold symmetry is associated with a well defined columnar growth mimicking the (clearly visible) pores and pore walls present in the alumina substrate (the NiO layer is the upper, brighter region of the layer). The height profiles measured across the pores, corresponding to Fig. 2(a)–(c), confirm that they are still open after the bilayer deposition (the finite transverse dimensions of the microscope tip and the occurrence of lateral tunnel as the tip enters the pore do not allow to follow the profile deep into the pores). An important issue is the trench separating each one of the six columns surrounding a pore, both in the NiO/Al_2O_3 and in the Fe/NiO deposits, as shown in the AFM images of Fig. 3(a) and (b), respectively (the Fe thickness corresponding to this figure is 20 nm). The trenches are, at least, 5 nm deep as quantified from the height profiles taken across pairs of those column tops (again the finite dimensions of the microscope tip and the occurrence of lateral tunnelling hinders a realistic evaluation of the trench depth).

Fig. 4 summarizes our results for the coercivity dependence on the temperature and Fe layer thickness, measured after field cooling the samples under 10 kOe, which was also

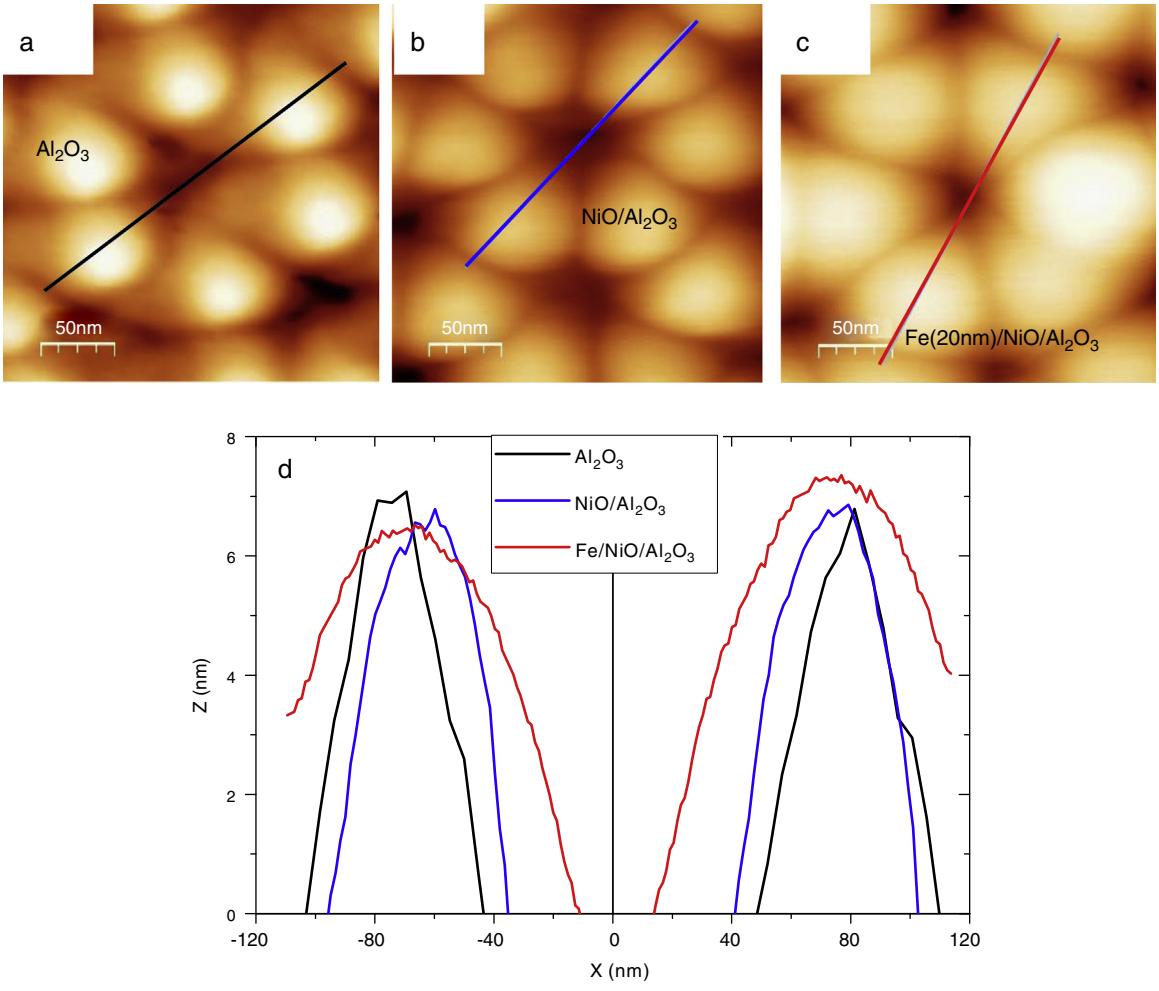

Fig. 2 – AFM images of the alumina substrate (a), NiO/Al_2O_3 (b) and $Fe/NiO/Al_2O_3$ (c) deposits. Height profiles corresponding to the three samples (d).

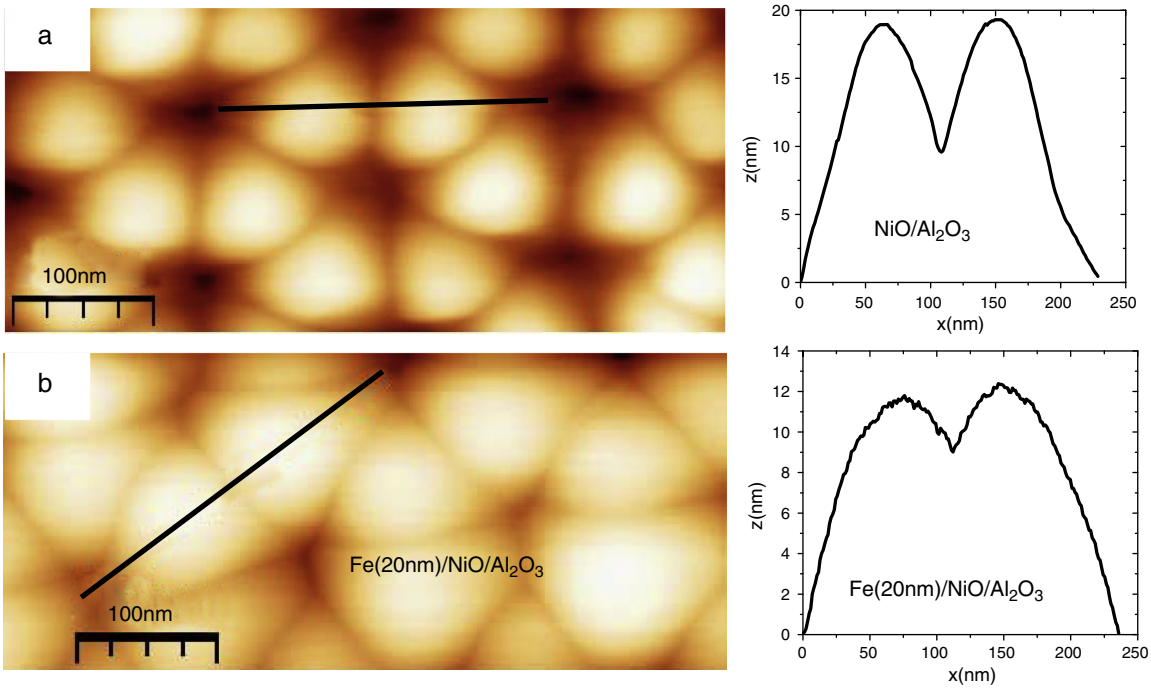

Fig. 3 – AFM images of neighbouring columns around the pores in the NiO/Al_2O_3 (a) and $Fe/NiO/Al_2O_3$ (b) deposits showing the trenches between them. The height profiles corresponding to the lines in (a) and (b) are shown on the right.

the maximum applied field for measuring the loops at all temperatures. From the figure it is possible to observe that the coercivity of the 5 nm Fe deposit increases sharply with decreasing temperature, from 250 Oe at 290 K, up to 750 Oe at 50 K. That range is mostly above the theoretical coherent rotation-based upper bound for the coercive force given by the anisotropy field $2K_1/M_S$ [8] (K_1 being the first order magnetocrystalline anisotropy constant and M_S the saturation magnetization of the considered phase). Explicitly, the anisotropy field of Fe is close to 550 Oe at room temperature and it increases to about 600 Oe at 50 K. Most important, the coercivity of Fe continuous films with thickness of the order of tens of nanometers is usually well below 100 Oe [9]. The large magnetic hardening of this sample can be attributed, first, to its thickness being less than 50% of the Fe correlation length, which ensures that all the Fe moments across the layer thickness are coupled to the interfacial AF moments created by the local symmetry breaking and, consequently, exhibiting high local anisotropies, especially at reduced temperatures. In addition, the layer deposited on top of the NiO columns has a thickness of 5 nm, below the AFM measured depth of the trenches (which, as already mentioned, is just a lower bound to the real trenches depth). This has as a plausible consequence the discontinuous morphology of the Fe deposit

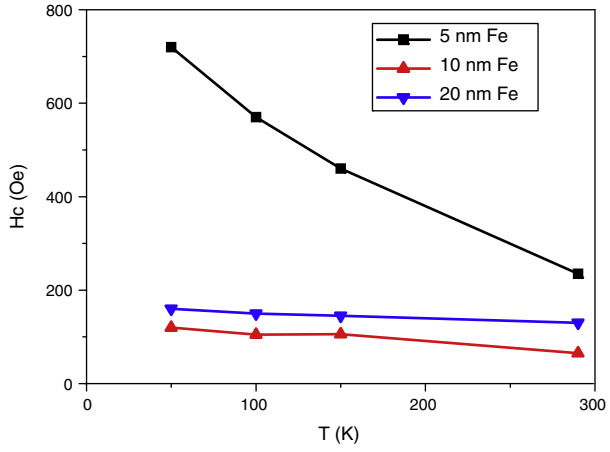

Fig. 4 – Coercivity as function of the temperature and Fe layer thickness, measured after field cooling the samples under an applied field of 10 kOe.

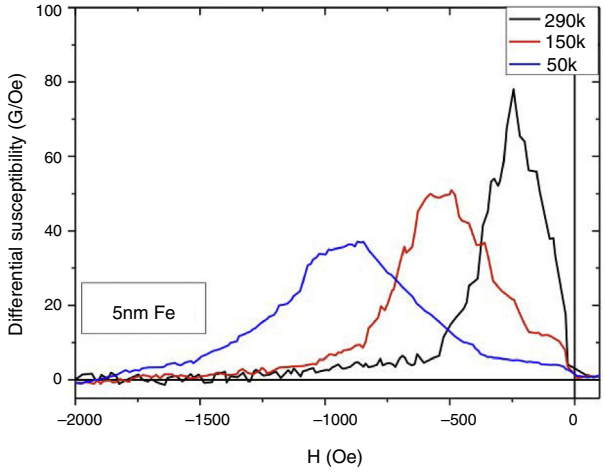

Fig. 5 – Differential susceptibility of the demagnetization branch of the loops measured at three temperatures in the bilayer with 5 nm Fe.

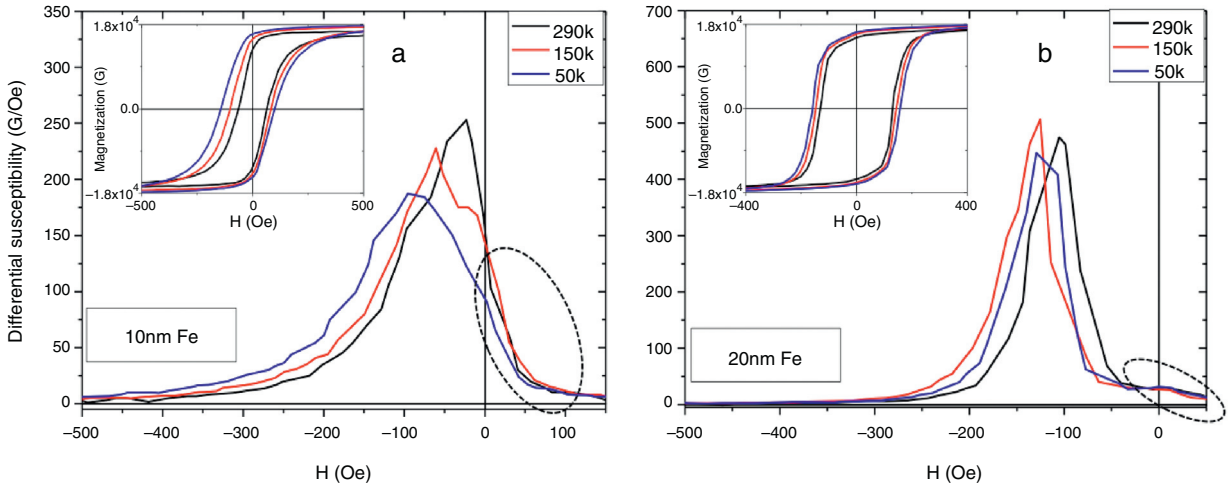

Fig. 6 – Differential susceptibility of the demagnetization branch of the loops (shown in each inset) measured at three temperatures in the bilayers with 10 nm (a) and 20 nm (b) Fe. The dotted areas in both graphs correspond to demagnetization events occurring at positive fields.

which, at least in the case of the Fe 5 nm sample, corresponds more to a hexagonally-packed set of dots than to a continuous film incorporating antidots. In order to confirm this view, we have plotted in Fig. 5 the differential susceptibility measured along the demagnetization branches of the hysteresis loops obtained at 50 K, 150 K and 290 K in the Fe 5 nm thickness sample. The demagnetization events are broadly distributed at all the temperatures and the width of that distribution increases with decreasing temperature. In particular, the differential susceptibility maximum at 50 K occurs at 860 Oe (that is 150 Oe above the sample coercive force) and has a width of 600 Oe, hardly attributable to any kind of collective process. Fig. 6(a) and (b) shows, respectively, the hysteresis loops (insets) and their corresponding differential susceptibility curves (demagnetization branch) of the Fe deposits 10 nm and 20 nm thick, at 50 K, 150 K and 290 K. As can be seen, the coercivity of these samples is much lower than that of the 5 nm deposit. This indicates that in these 10 and 20 nm Fe samples the coercive force is still linked to the F/AF interfacial coupling but that some coercivity deteriorating effects occur in them. The deteriorating effect cannot exclusively be identified as related to the increase in the Fe layer thicknesses since their values in these samples are still clearly lower than the single crystal Fe Bloch domain wall width, $\delta_{w\,Fe} = \pi l_{ex} = 38$ nm [6]. Considering this, a possible nucleation process taking place at the lower anisotropy regions of the samples (that is, the region near the capping layer/Fe interface) could not easily propagate across the sample. The field dependence of the differential susceptibility allows to gain additional information on the origin of the coercive force deterioration. As it is evident from Fig. 6, and similarly to the case of the Fe 5 nm sample, the distribution of demagnetizing events in the 10 nm deposit is still broad, with a half maximum width (from 130 Oe at 290 K to 225 Oe at 50 K, approximately) slightly above the corresponding coercivity value at each temperature. In contrast with the case of the Fe 5 nm sample, a remarkable first quadrant demagnetization can be detected for both the 10 nm and 20 nm samples, associated to the coercivity decrease. We suggest that these regions demagnetizing at positive fields should be identified as corresponding to Fe grains partially covering (and partially obstructing) the walls of the NiO/Al_2O_3 pores, since in those regions the local Fe magnetization would presumable be directed, at low positive fields and due to shape effects, perpendicularly to the applied field. It is important to note that the differential susceptibility peaks of the 20 nm Fe sample are about twice as high as those of the 10 nm deposit and they are also much narrower, with half maximum widths below 100 Oe. Thus, we can conclude that the demagnetization of this sample tends to be collective to a higher extent. This might be linked to the fact that a Fe thickness of 20 nm can bridge the gap in between the Fe dots (ca. 5 nm) at the top of the NiO/Al_2O_3 columns.

Finally, in Fig. 7 we show the temperature dependence of the loop shift measured in all the samples (see also the

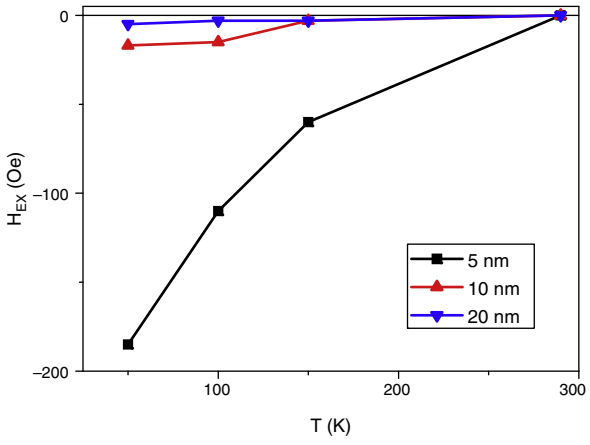

Fig. 7 – Temperature dependence of the exchange bias (loop shift) measured in the three Fe deposits.

insets in Fig. 6). That shift is a measure of the net polarization of the interfacial AF unbalanced moments whose direction is not modified by demagnetizing fields of the order of the global sample coercive force. As a general trend, the exchange bias shift and the coercivity decrease with increasing F layer thickness in exchange biased systems. This is related to the limited distance influenced by the interfacial F/AF coupling [2]. Accordingly, the loop shift in the 10 and 20 nm Fe layer samples is reduced with respect to that of the 5 nm Fe deposit, although a strong contribution to the coercivity reduction in the former samples may result from the occurrence in these thicker Fe layers of regions having mutually perpendicular magnetization.

Conclusions

We have analyzed the combined effects of the F/AF interfacial effects and of the morphology on the magnetic behaviour of a series of the Fe/NiO layers, with different Fe layer thicknesses, deposited on porous alumina membranes. We have shown that the deposits, preserving the porous structure of the membrane, present a columnar structure. The wall around each pore is hexagonal and it is formed by six columns separated by trenches. The coercivity of the deposits is strongly dependent on the Fe layer thickness. For the 5 nm sample the coercivity is of the order or above the anisotropy field of Fe and the switching fields present a broad distribution, as a result of the interfacial anisotropy affecting the whole sample thickness and also of the dot-like behaviour of the Fe deposited on top of each column. The 10 nm and 20 nm thick Fe deposits have a much lower coercivity and, in the case of the 20 nm sample, a narrow distribution of demagnetization events, related to a demagnetization process which is collective to a greater extent, related to the partial filling of the pores and the trenches in between the Fe at the top of the NiO columns. The presence of the Fe/NiO interface leads to the appearance of the exchange bias effect, that, as expected is negligible for the thickest film due to its thickness being above the Fe exchange correlation length [2].

Acknowledgements

Work supported by the Spanish MINECO (Ministerio de Economía y Competitividad) under Projetcs MAT2013-47878-C2-1-R and MAT2013-47878-C2-2-R.

REFERENCES

[1] J.W. Lau, J.M. Shaw, Magnetic nanostructures for advanced technologies: fabrication, metrology and challenges, J. Phys. D: Appl. Phys. 44 (2011) 303001, http://dx.doi.org/10.1088/0022-3727/44/30/303001.
[2] J. Nogués, J. Sort, V. Langlais, V. Skumryev, S. Suriñach, J.S. Muñoz, M.D. Baró, Exchange bias in nanostructures, Phys. Rep. 422 (2005) 65–117.
[3] F. García-Sánchez, E. Paz, F. Pigazo, O. Chubykalo-Fesenko, F.J. Palomares, J.M. González, F. Cebollada, J. Bartolomé, L.M. García, Coercivity mechanisms in lithographed antidot arrays, Europhys. Lett. 84 (2008) 67002, http://dx.doi.org/10.1209/0295-5075/84/67002.
[4] E. Paz, F. Cebollada, F.J. Palomares, J.M. González, M.-Y. Im, P. Fischer, Scaling of the coercivity with the geometrical parameters in epitaxial Fe antidot arrays, J. Appl. Phys. 111 (2012) 073908, http://dx.doi.org/10.1063/1.3702584.
[5] A.M. Goodmann, K. O'Grady, H. Laidler, N. Owen, X. Portier, A.F. Petford-long, F. Cebollada, Magnetization reversal processes in exchange-biased and spin-valve structures, IEEE Trans. Mag. 37 (2001) 565–570.
[6] R. Skomski, Nanomagnetics, J. Phys.: Condens. Matter 15 (2003) R841–R896.
[7] A. Gutierrez, G. Dominguez-Canizares, J.A. Jimenez, I. Preda, D. Diaz-Fernandez, F. Jimenez-Villacorta, G.R. Castro, J. Chaboy, L. Soriano, Hexagonally-arranged-nanoporous and continuous NiO films with varying electrical conductivity, Appl. Surf. Sci. 276 (2013) 832–837, http://dx.doi.org/10.1016/j.apsusc.2013.04.007.
[8] J.M.D. Coey, Magnetism and Magnetic Materials, Cambridge University Press, Cambridge, 2010, pp. 171.
[9] F. Cebollada, A. Hernando-Mañeru, A. Hernando, C. Martínez-Boubeta, A. Cebollada, J.M. González, Anisotropy, hysteresys, and morphology of self-patterned epitaxial Fe/MgO/GaAs films, Phys. Rev. B 66 (2002) 174410, http://dx.doi.org/10.1103/PhysRevB.66.174410.